Denoising ECG Signals by Applying Discrete Wavelet Transform

Áron Fehér
Department of Electrical Engineering
Sapientia Hungarian University of Transylvania
Targu Mures, Romania
Email: fehera@ms.sapientia.ro

***Abstract*—This work introduces an ECG signal denoising method using discrete wavelet transforms. In the first part of the study, classical denoising methods were revised, tested and analyzed. To minimize signal distortion and resource usage the wavelet decomposition and thresholding was proposed. In the second part of the study, the methods mentioned above were used to remove the baseline wondering and high-frequency noise components of the acquired ECG signal. Simulations are presented in Matlab based on professional pre-recorded raw EKG signals. Experimental results, using a self-developed ZYNQ SoC based data acquisition system, are also shown to illustrate the applicability of the proposed signal processing methods.**

***Keywords*—** Digital Signal Processing, Filtering Algorithms, Discrete Wavelet Transforms, Signal Denoising, Electrocardiography

I. Introduction

Nowadays, where nearly anybody can have at least one smart device, the amount of physical exercise a man makes is steadily decreasing, while the consumption of sugary and fatty food is, at best, constant, or increasing. As a consequence, the amount of people with heart diseases increases rapidly. While the best way to avoid such conditions is to change the way of one's living completely, the easiest, fastest way is to monitor one's health status at least periodically.

To successfully diagnose the health condition, specialized equipment and data processing are needed. Electrocardiography is the process of monitoring the heart's electrical activity over a period by placing electrodes on the skin. A single cycle of the electrocardiogram represents the successive atrial and ventricular depolarisation and repolarisation. An ideal ECG signal is shown in Fig 1, where the first graph shows the ECG signal in the time domain with its characteristic intervals, while the second graph shows the same ECG signal in the frequency domain using the discrete Fourier-transform. On the frequency graph, we can see the complexity of a clean ECG signal. The ECG signals being very sensitive and weak in nature are highly prone to even small noise, some of the typical interferences are baseline wander (BLW), power line interference (PLI), electromyographic noise and electrosurgical noise.

Filtering is the way of removing undesired signals (noises) from the primary signal. For every well distinguishable noise,

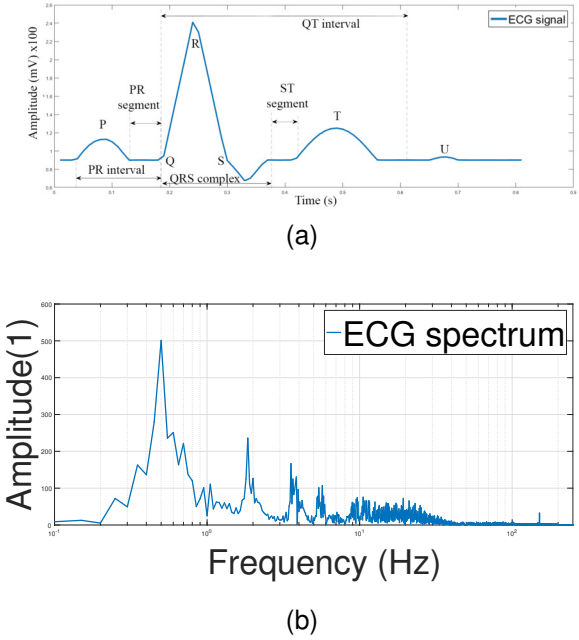

Fig. 1. An ideal ECG signal in time (a) and frequency (b) domain.

of PLI, while in [2] the removal of the baseline wondering was studied.

II. Noises contaminating the ECG signal

A. Power Line Interference

The PLI of 50 Hz (and harmonics) is the source of inference. This inference is caused by poorly shielded nearby machinery's electromagnetic field, the stray effect of alternating current fields due to cable loops and/or trace loops on the ECG circuit, improper grounding of ECG machine or patient, etc.

As it is shown in Fig 1, the ideal ECG signal has important information at 50 Hz and above, so leaving the PLI or cutting out the frequency band above 50 Hz will distort the signal (especially the QRS complex).

B. Base line wondering

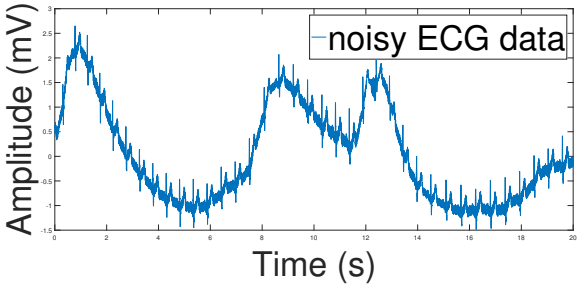

Fig. 2. ECG signal contaminated with PLI and BLW noises.

moving cables, patient movement, loose electrodes, or the change of skin impedance due to sweating [3], etc. This artifact is manifested as a low-frequency additive noise.

III. Wavelet Transform Based Filtering

A. The wavelet transform

The classic operation to transform a stationary signal from time domain to frequency domain was the Fourier transform shown in (1).

$$X(f) = \int_{-\infty}^{\infty} x(t) e^{-2\pi j f t} dt \tag{1}$$

The downside of the Fourier transform is the loss of the time domain properties; another downside is that the transform gives reliable results only if it is applied to stationary signals. The short-time Fourier transform (STFT) was developed to show accurate time-frequency representation, see [4]. The time resolution must be increased with the central frequency of the analysis filter to counter the resolution limitation of the STFT. This resolution change at different frequencies is obtained by *Wavelet packets*. The continuous wavelet transform (CWT) is a linear operation that follows the mentioned ideas, while all impulse responses of the filter bank are defined as scaled versions of the prototype. The equation (2) shows the CWT operation, where *x(t)* is the signal in time domain, while *h(t)* is the mother wavelet 3, with wavelets delayed τ, and dilated a. Some of the wavelets used for the CWT are Poisson, Morlet, Ricker, and Meyer wavelets, see for example in [5], [6], [7].

$$CWT_x(\tau, \alpha) = \frac{1}{\sqrt{\alpha}} \int_{-\infty}^{\infty} x(t) h(\frac{t-\tau}{\alpha}) dt \tag{2}$$

B. The discrete wavelet transform

The discrete wavelet transform (DWT) uses filter banks for the construction of the multiresolution analysis, which improves computation efficiency. As shown in Fig 4, the wavelet transform computation requires a pair of filters. One of the pairs calculates the wavelet coefficients, and the other applies the scaling function. This scaling function, implemented with filter coefficients LPF (the scaling function behaves as a low-pass filter), provides the approximation of the signal, while the wavelet function (HPF - behaves as a high-pass

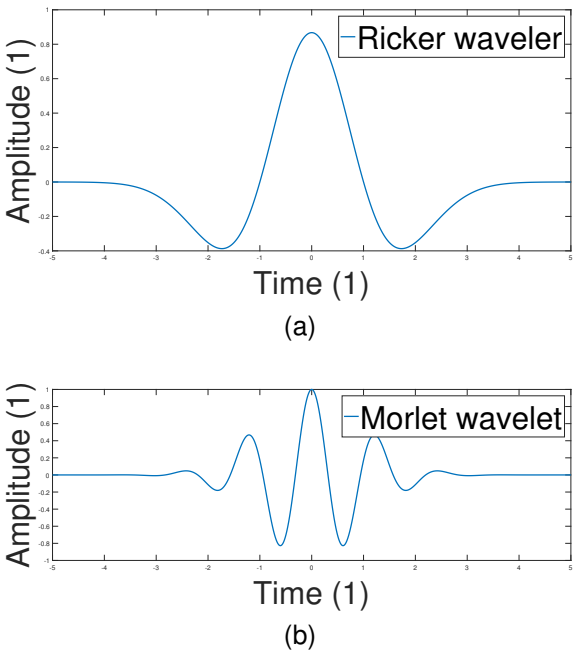

Fig. 3. Ricker (Mexican hat) and Morlet continuous wavelets.

wavelet filter coefficients are given by the chosen mother wavelet, the scaling and wavelet filters (LPF and HPF) are related by equation 3, where *LPF* is the wavelet or lowpass filter vector, *HPF* is the scaling or highpass filter vector, *L* is the length of the vector, while k is the numeral of elements $k = \overline{0..(L-1)}$. Besides the filtering, downsampling is used (by the factor of 2). When a signal has passed through the two filters and down-sampled, the result is called one level wavelet transform. The results are the detail coefficients *(d)* and average coefficient *(a)*. These coefficients are used for signal filtering and compressing [8].

$$HPF[k] = (-1)^k LPF[L-k] \tag{3}$$

If the data rate of the input signal is *Ts*, then the data rate of the coefficients will be as it is shown in Table I, in the case of a level 3 decomposition see (Fig 4).

TABLE I
Data Rate of the Output Coefficients of the Three-Level DWT Decomposition.

Levels	Level 0 x[n]	Level 1 d1[n]	Level 2 d2[n]	Level 3 d3[n]	Level 3 a3[n]
Rates	Ts	Ts/2	Ts/4	Ts/8	Ts/8

The discrete wavelet reconstruction or inverse wavelet transform (IDWT) has the same structure, but the down-sampling is replaced by up-sampling.

C. Wavelet thresholding

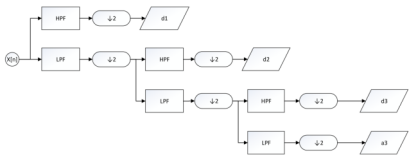

Fig. 4. Wavelet tree (Mallat's algorithm) of DWT for a three-level decomposition.

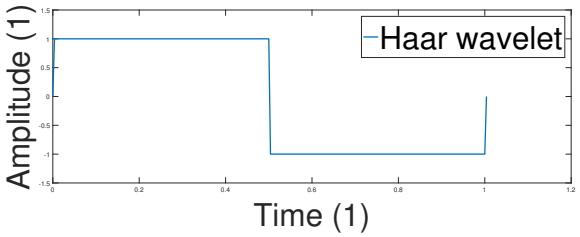

(a)

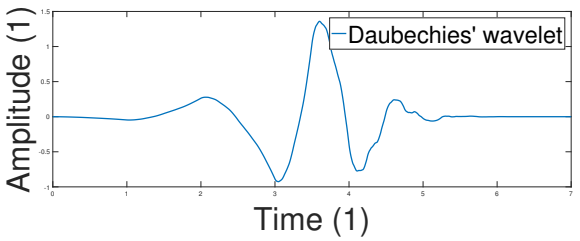

(b)

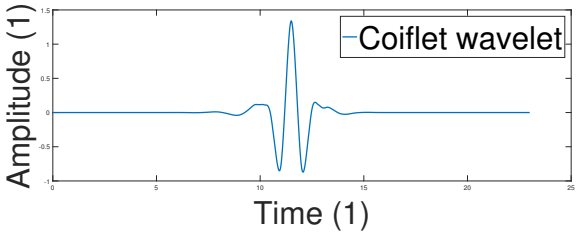

(c)

Fig. 5. In this figure some discrete wavelets are shown: The basic Haar wavelet(a), Daubechies' wavelet (b), and Coiflet wavelet

transformation, and it will be present in every wavelet coefficient. The wavelet coefficients of a signal are sparse, so most of the coefficients of a noiseless signal are close to zero. Therefore the problem of recovering the noiseless signal can be reformulated as one of recovering the coefficients that are stronger than the noise background. This can be done by *thresholding*.

Thresholding is a nonlinear, diagonal operator, which only passes through the input signal if the amplitude is greater than a given value (threshold). The most important thresholding operators are hard (4) and soft thresholding (5). Soft thresholding

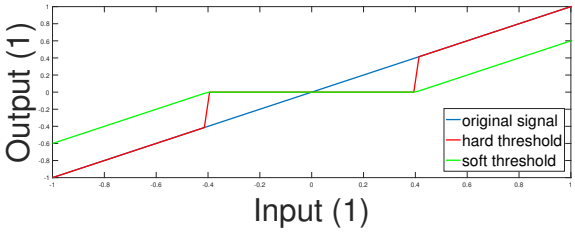

Fig. 6. Hard and soft threshold representation on a linear input signal.

$$\theta_\lambda^0(x[k]) = \begin{cases} x[k], & \text{if } |x[k]| > \lambda \\ 0, & \text{otherwise} \end{cases} \tag{4}$$

$$\theta_\lambda^1(x[k]) = max\left(0, 1 - \frac{\lambda}{|x[k]|}\right) \tag{5}$$

Most of the algorithms try to estimate the optimal value of λ (Minimax algorithm [9]), with the help of the noise level. Another method for determining the threshold level was proposed in [10], the scheme was based on the explicit form of *Stein's unbiased risk estimate* (SURE) - (6), where *Crd* denotes cardinality. The threshold λ should be chosen by minimizing SURE (7).

$$SURE(\lambda, x) = n + \sum_{i=1}^{n}[min(|x[i]|, \lambda)]^2 - 2 * Crd(i : |x[i]| < \lambda) \tag{6}$$

$$\lambda^* = argmin_{0 \le \lambda \le \sqrt{2log(n)}} SURE(\lambda, x) \tag{7}$$

According to [10] the final form of the threshold should be chosen as shown in (9), where $\nu_s(x)$ is the sparsity of the coefficients shown in (8).

$$\lambda_{ShureShrink}(x) = \begin{cases} \sqrt{2log(n)}, & \text{if } \nu_s(x) \le 1 \\ \lambda^*, & \text{otherwise} \end{cases} \tag{8}$$

$$\nu_s(x) = s^{-\frac{1}{2}} \frac{\sum_{i=1}^{n}(x^2[i] - 1)}{log_2^{\frac{3}{2}} n} \tag{9}$$

IV. The Application of DWT to ECG Filtering

The DWT based filtering of a signal is done with the signals detail and average coefficients, so the first step is to generate the wavelet coefficients. The second step is to scale the coefficients based on the thresholding methods mentioned above. The final step is to recreate the signal from the coefficients with IDWT.

- To generate the wavelet coefficients the DWT is applied conform Mallat's algorithm shown in Fig 4. The HPF and LPF kernels can be generated while choosing the appropriate mother wavelet. The Haar wavelet (Fig 5,

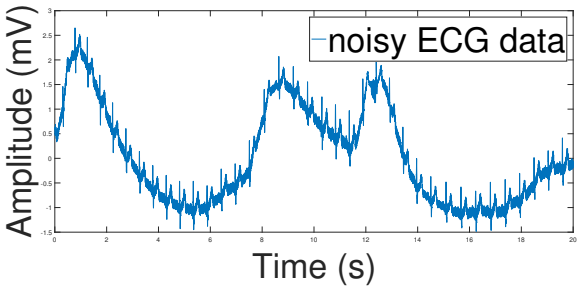

Fig. 7. ECG signal with BLW, PLI, and HF noises added.

Fig. 8. Complete ECG signal filtering system with cascaded filter blocks.

memory efficient. It uses only two scaling and wavelet coefficients, thus calculate pairwise averages and differences, in other words, it only reflects changes in adjacent data pairs. The Daubechies (Fig 5,b) wavelet is orthogonal and has compact support characteristics. The wavelet uses an overlapping window, the average and difference are generated from more than 2 data points making it smoother than the Haar wavelet. The Symlet or Coiflet (Fig 5,c) wavelets differ from the Daubechies wavelet by increased computational overhead. These wavelets are the least asymmetric wavelets.

- After generating the average and detail coefficients, the scaling algorithm is applied based on the noise present in the system (Minimax or SURE algorithms).
- The scaled coefficients can be used to create the filtered signal by applying the IDWT with MALLAT's algorithm based on the mother wavelet chosen in the first step.

To denoise an ECG signal, the upper mentioned steps can be used in the following form:

1) Store the raw data(the storage size should be the power of 2).
2) Choose a mother wavelet.
3) Generate the wavelet coefficients with DWT.
4) Remove the BLW noise by scaling the average coefficient.
5) Remove the PLI and HF noises by applying SURE algorithm to the detail coefficients.
6) Generate the filtered data from the coefficients with IDWT.

V. The Comparison of Different Filtering Methods

To test the classic and modern filtering algorithm, a custom made signal and a pre-filtered ECG signal was used from Physio Bank ATM [11] and imported into Matlab. The ideal ECG signal was combined with additive noises: a sine wave of 15 mHz for BLW, a sine wave of 50 Hz for PLI, and a uniformly distributed noise with a frequency band of 300 Hz to 500 Hz for HF noise as shown in Fig 7. To compare the filters, the Mean Squared Error (MSE) and the Signal to Noise Ratio (SNR) was used as shown in (10), where ω is the noise,

$$SNR(x,\omega) = 10lg\left(\frac{\sum \|FFT(x)\|}{\sum \|FFT(\omega)\|}\right) \tag{10}$$

A. Classic filtering

When classic filters are used, each response type from to one filter: The BLW noise has to be removed with a high-pass filter, The PLI noise has to be removed with a bandstop filter, while the high-frequency noises have to be removed with a low-pass filter as shown in Fig 8.

The first tested filtering structure was a FIR approach. The BLW removal was achieved with a 2000th order Equiripple filter with a density factor of 20, stop frequency of 0.01 Hz and pass frequency of 0.5 Hz. The PLI was removed with an 1114th order Equiripple filter with a density of 20 Hz, passbands from DC to 48 Hz and from 52 Hz to the Nyquist frequency (or *fs*/2, where *fs* is the sampling frequency), and a stopband from 49 Hz to 51 Hz. The high-frequency noises were removed with a 254th order Nuttall low-pass filter with cut-off frequency of 250 Hz.

As shown in Fig 9, the filters removed the noise artifacts, but they induce a small delay, and a distortion until the FIR convolution registers are full with data (approx. 2s). The SNR increased to 24.1539 dB.

The second applied filtering structure was a complete IIR approach. The BLW removal was achieved with a 3rd order Butterworth high-pass filter. The PLI was removed with a 24th order bandstop Butterworth filter, and the high-frequency noises were removed with a 31st order Butterworth filter. The stop and pass frequencies were the same as in the case of FIR filters.

As shown in Fig 10, the filters removed the BLW, and high-frequency noises, but had some residual noise from the PLI, but the distortion and delay was minimized due to the small convolution registers. The SNR of the filtered signal was 20.4868.

B. DWT based ECG filtering

To filter the signal, a mother wavelet must be chosen. For this research, the symlet 8 wavelet was used. Since the sampling frequency is 1 kHz, to remove the BLW, a 10th order decomposition was necessary. The filtering is done as

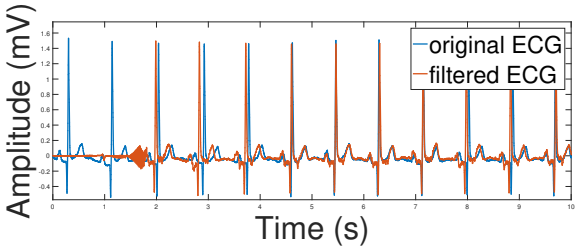

Fig. 9. ECG signal filtered with FIR high-pass, band-stop, and low-pass filter stages.

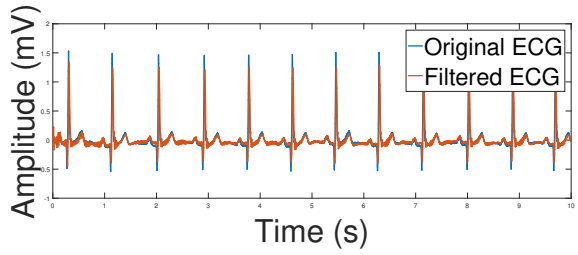

Fig. 10. ECG signal filtered with IIR high-pass, band-stop, and low-pass filter stages.

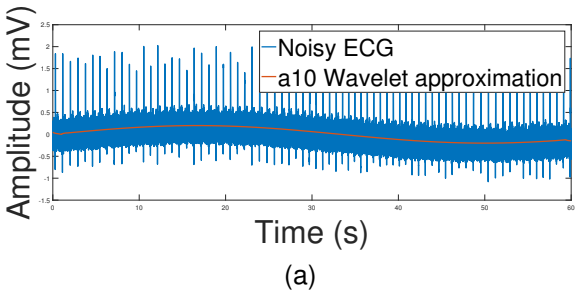

Fig. 11. In figure (a) the noisy ECG signal is shown with the 10th order wavelet approximation, while in figure - the artificial BLW sine function is reconstructed (b) the original ECG signal is compared with the filtered ECG signal.

average coefficient a10 are calculated). The average coefficient contains only the BLW as shown in Fig 11 (a), so it will be set to 0, while the detail coefficients will be thresholded with the soft SURE method. After thresholding, a wavelet reconstruction is used to generate the filtered data. The result can be seen in Fig 11 (a), and the SNR was 30.5355 dB,

TABLE II
SNR OF THE ECG SIGNAL WITH THE DIFFERENT FILTERING METHODS.

Filter algorithm	Algorithm complexity	SNR (dB)	MSE (mV)
Raw signal	-	6.8134	-
All FIR filters	$O(N) = Nlg(N)$ 2000, 1114, 245 taps	24.1539	0.0847
All IIR filters	$O(N) = Nlg(N)$ 3, 24, 31 order	20.4868	0.0249
Wavelet thresholding	$O(N) = Nlg(N)$ 10,10	30.5355	$9.42 * 10^{-4}$

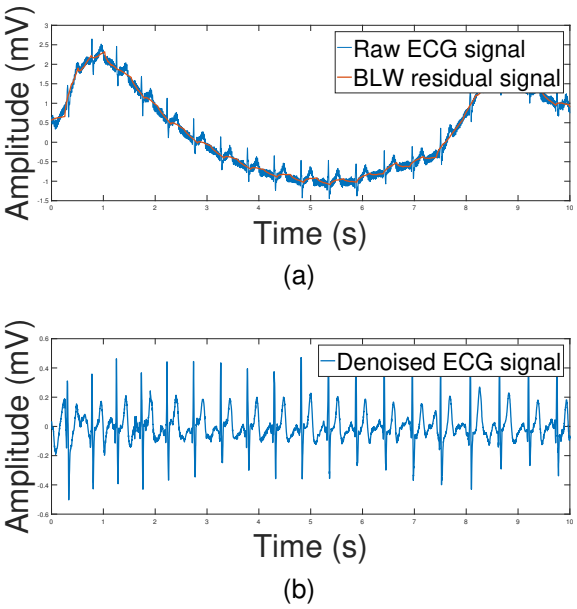

Fig. 12. In figure (a) The raw ECG signal sampled with the SoC is shown, and the BLW residual signal from the first part of the filtering algorithm,while in figure (b) the filtered signal is shown.

VI. EXPERIMENTAL RESULTS

The proposed method was implemented in a ZYNQ7 SoC (System on Chip) form Xilinx. This SoC has a Programmable Logic section (PL) and a Processing System Section (PS) embedded together. An IP core was generated with HDL coder based on the wavelet filtering method mentioned above (written in C++). The IP Core was then exported to Vivado and tested on real-time data. The hardware was designed as follows (shown in Fig 13):

1) The PS acquires data from the SPI ADC (Analog to Digital Converter) and sends the data to the filtering IP.
2) The filtering IP in the PL pushes the data into a 2048 element register, applies the first DWT/IDWT pair to remove the BLW, then applies the second DWT/IDWT with thresholding to remove the PLI and HF noises. After the filtering is done, the data is sent back to the PS.
3) The PS sends both the clean and noisy data to the PC through UART communication, where it can be

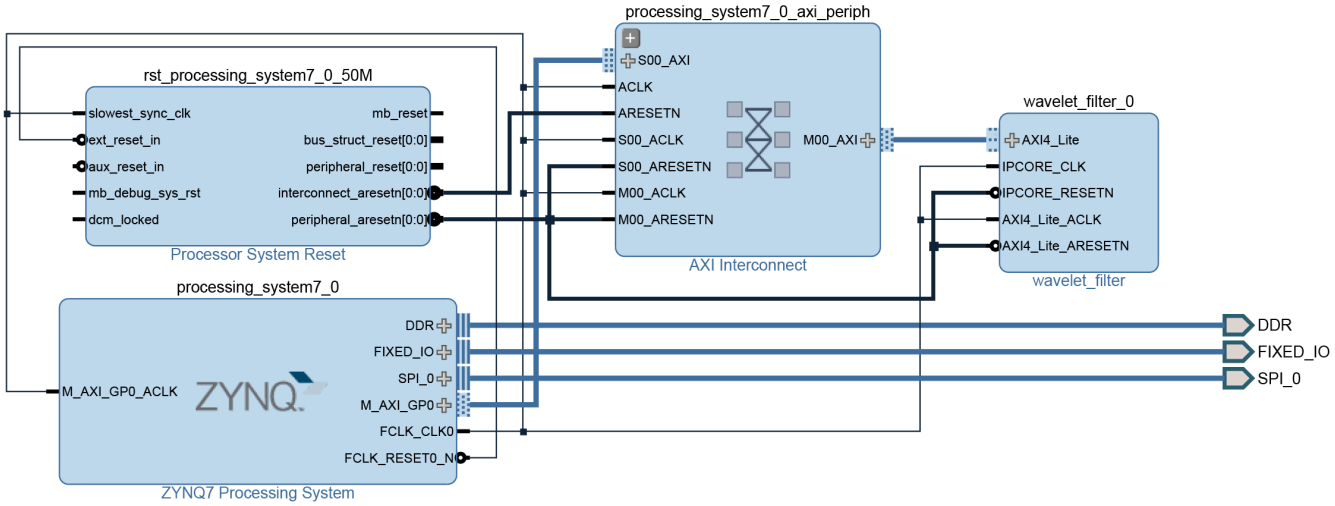

Fig. 13. The hardware implementation of the Wavelet denoising algorithm. The Zynq PS receives the ECG data on the SPI bus and uses the PL IP as a hardware accelerator.

The SNR, MSE can be further improved with further studying different mother wavelet properties and thresholding methods. The implemented IP core manages to filter the signal under 8 ns, with 200 MHz PL clock source, but the processing time can further be improved by pipelining the algorithm, unrolling loops, and using Stream interface with DMA (Direct Memory Access) instead of AXI Lite interface.

VII. Conclusion

The proposed Wavelet thresholding method not only successfully removed the BLW, PLI, and HF noises from the sampled ECG signals. A SoC hardware implementation was proposed to verify the usability of the algorithm, based on which the favorable conclusion is drawn, the algorithm can be implemented in hardware and can be used in real time, requires less computation than conventional FIR and IIR filters and the same attenuation can be achieved with less filtering stages.

References

[1] M. Meidani and B. Mashoufi, "Introducing new algorithms for realising an fir filter with less hardware in order to eliminate power line interference from the ecg signal," *IET Signal Processing*, vol. 10, no. 7, pp. 709–716, 2016.

[2] T. Singh, P. Agarwal, and V. K. Pandey, "Ecg baseline noise removal techniques using window based fir filters," in *Medical Imaging, m-Health and Emerging Communication Systems (MedCom), 2014 International Conference on*, Nov 2014, pp. 131–136.

[3] B. Taji, S. Shirmohammadi, V. Groza, and I. Batkin, "Impact of skin electrode interface on electrocardiogram measurements using conductive textile electrodes," *IEEE Transactions on Instrumentation and Measurement*, vol. 63, no. 6, pp. 1412–1422, June 2014.

[4] O. Rioul and M. Vetterli, "Wavelets and signal processing," *IEEE Signal Processing Magazine*, vol. 8, no. 4, pp. 14–38, Oct 1991.

[5] S. Mustafa, A. Abbosh, B. Henin, and D. Ireland, "Brain stroke detection using continuous wavelets transform matching filters," in *2012 Cairo International Biomedical Engineering Conference (CIBEC)*, Dec 2012, pp. 194–197.

[6] A. N. Saatlo and S. Ozoguz, "Cmos implementation of scalable morlet wavelet for application in signal processing," *in 2015 38th International*

[7] V. J. Samar, H. Begleiter, J. O. Chapa, M. R. Raghuveer, M. Orlando, and D. Chorlian, "Matched meyer neural wavelets for clinical and experimental analysis of auditory and visual evoked potentials," in *1996 8th European Signal Processing Conference (EUSIPCO 1996)*, Sept 1996, pp. 1–1.

[8] B. A. Rajoub, "An efficient coding algorithm for the compression of ecg signals using the wavelet transform," *IEEE Transactions on Biomedical Engineering*, vol. 49, no. 4, pp. 355–362, April 2002.

[9] D. L. Donoho and I. M. Johnstone, "Ideal spatial adaptation by wavelet shrinkage," *Biometrika*, vol. 81, pp. 425–455, 1994.

[10] ——, "Adapting to unknown smoothness via wavelet shrinkage," *JOURNAL OF THE AMERICAN STATISTICAL ASSOCIATION*, pp. 1200–1224, 1995.

[11] A. L. Goldberger, L. A. N. Amaral, L. Glass, J. M. Hausdorff, P. C. Ivanov, R. G. Mark, J. E. Mietus, G. B. Moody, C.-K. Peng, and H. E. Stanley, "PhysioBank, PhysioToolkit, and PhysioNet: Components of a new research resource for complex physiologic signals," *Circulation*, vol. 101, no. 23, pp. e215–e220, 2000 (June 13), circulation Electronic Pages: http://circ.ahajournals.org/content/101/23/e215.full PMID:1085218; doi: 10.1161/01.CIR.101.23.e215.